SENSITIVITY OF PERTURBATION GROWTH TO FLOW CHARACTERISTICS AND SAMPLING STRATEGY

C. Hohenegger [1], C. Schär[1]

[1] Institute for Atmospheric and Climate Science, ETH, Winterthurerstr. 190, 8057 Zürich, Switzerland
E-mail: *hohenegger@env.ethz.ch*

Abstract: The chaotic nature of the weather/climate attractor intrinsically limits the deterministic skill of weather forecasts by promoting rapid growth of errors. In this study, such error growth is simulated by artificially perturbing the atmosphere at initial time, and its sensitivity to the chosen perturbation methodology and to the flow characteristics is investigated. The different simulations are integrated with the limited-area model LM run on a convection-resolving grid. Results demonstrate that the locations of growing disturbances are insensitive to the definition of the initial temperature perturbation. This can be explained through an analysis of the perturbation growth and propagation mechanisms. In particular, rapid radiation of the imposed initial disturbance through a sound wave and presence of specific flow characteristics (e.g. convective instability) appear to force localized error growth far remote from the initial perturbation.

Keywords *– Predictability, error growth and propagation, Ensemble Prediction System (EPS)*

1. INTRODUCTION

The skill of deterministic weather forecasts is limited by the rapid growth of small-amplitude errors projected on the chaotic climate/weather attractor. Error growth may arise from uncertainties in the initial conditions and may be taken into account by perturbing the initial state of the atmosphere, a technique widely used for the generation of EPS (see e.g. Ehrendorfer 1997). While the benefits of such probabilistic approaches are now recognized, opinions diverge on the optimal choice of the ensemble members' initial conditions. This is particularly the case for short-range high-resolution forecasts, where the mechanisms promoting error growth and propagation are not well known.

In this study, the sensitivity of short-range limited-area weather forecasts to a set of initially introduced temperature perturbations and to the flow characteristics is investigated. The results of the different simulations are compared and explained through an analysis of the growth and propagation of small-amplitude errors.

The simulations are performed with the Lokal Modell (LM, see Steppeler et al. 2003) run on a convection-resolving grid of 2km for the three MAP cases IOP2a (from 16.09.99 21UTC to 18.09.99 6UTC), IOP2b (from 19.09.99 21UTC to 21.09.99 6UTC) and IOP3 (from 24.09.99 21UTC to 26.09.99 6UTC). The LM model has been shown (see Hohenegger and Schär 2005a) to successfully reproduce the typical features (e.g. precipitation pattern and intensity) associated with those three cases. The different simulations are obtained by adding at initial time Gaussian perturbations of variable structures (width, amplitude, depth and location) to the temperature field of a control simulation under use of identical lateral boundary conditions (i.e. perfect predictable synoptic situation).

2. RESULTS

2.1. Sensitivity to sampling strategy

Fig. 1 shows the vertically integrated absolute temperature difference between perturbed and control simulations valid at 22UTC on the 17.09.99 (IOP2a). The initial Gaussian temperature disturbances which lead to Fig. 1a and 1b distinguished themselves in their location (see the dotted lines on Fig. 1), magnitude (1K against 4 K), sign (positive against negative), half width (88 km against 123 km) and

depth (approximately 80m against 2km). Despite this, Fig. 1a and 1b show a surprisingly high level of agreement. Both maps pinpoint to an enhanced discrepancy over the Piedmont region, parts of Switzerland, Bavaria and the French Jura chain. The characteristics of the imposed Gaussian disturbances seem to affect the magnitude of the induced temperature differences, not their location (i.e. the regions showing a loss in deterministic skill seem highly predictable). Considerations of other synoptic situations and predictability levels, as given through the simulations of IOP2a, IOP2b and IOP3, and of other model variables lead to similar conclusions (see Hohenegger and Schär 2005a): Larger discrepancies appear in the magnitude of the triggered disturbances, not in their location.

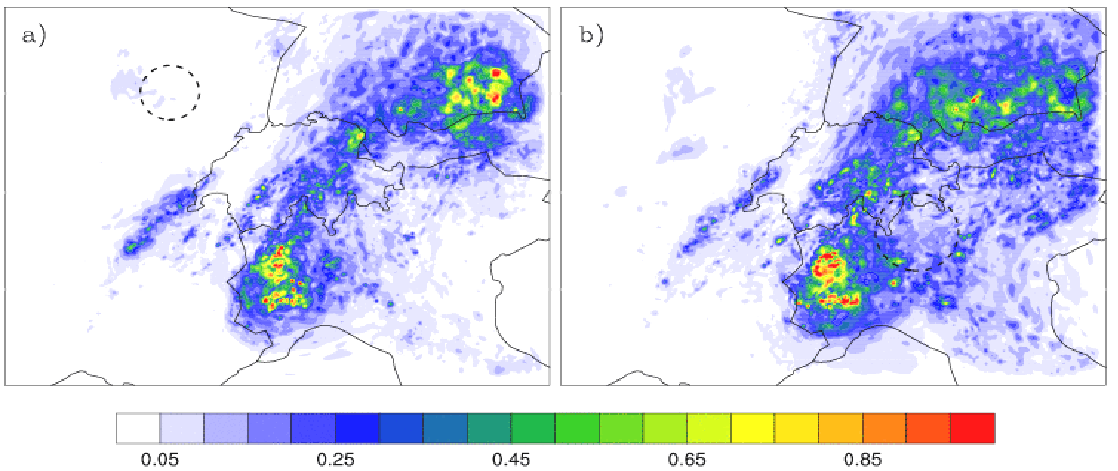

Figure 1. Vertically integrated absolute temperature difference between perturbed and control simulations obtained with two different initial Gaussian disturbances (location is dotted) for the 17.09.99 at 22 UTC.

The obtained correlation between the simulations is further illustrated with Fig. 2, in relation with the question of the linearity of the system. Fig. 2 shows time series of the correlation coefficient calculated between initially twin (positive and negative) perturbations for the three MAP cases. Higher correlations, in the order of 0.95, could be obtained by computing the vertically integrated ranked correlation coefficient. Fig. 2 illustrates a rapid decrease of the anticorrelation in the first simulation hours, indicating the predominance of nonlinear effects. This process is quicker in IOP2b than in IOP3 and IOP2a. The duration of the linear regime is mainly determined by the degree of overlapping between the locations of the initial disturbances and of the instabilities (see also Walser et al. 2004).

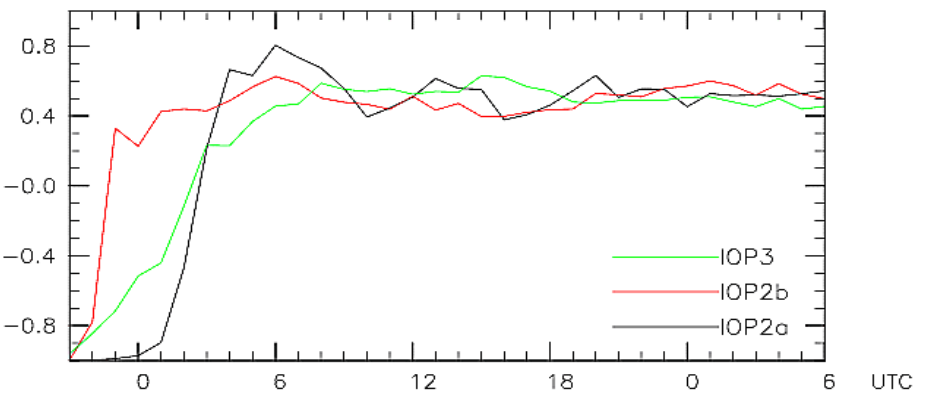

Figure 2. Correlation coefficient between twin (positive and negative) initial perturbations for the three MAP cases.

2.2. Error growth and propagation

The observed insensitivity might be related to the mechanisms promoting error growth and propagation. Fig. 3a shows in that context a log-plot of the vertical maximum absolute temperature difference between perturbed and control simulations averaged over the Simplon region, which was characterized by convective instability in IOP2a. The location of the Simplon region (black box) and of the initial Gaussian disturbances (dashed green and dashed red circle) leading to the two curves on Fig. 3a can be found on Fig. 3b. The distinctive initial positions (and characteristics) of the green and red disturbances explain the large discrepancy obtained during the first simulation hours (see Fig. 3a). The differences are nevertheless rapidly smoothed out with time due to the saturation of the red curve for an exponential increase of the green curve.

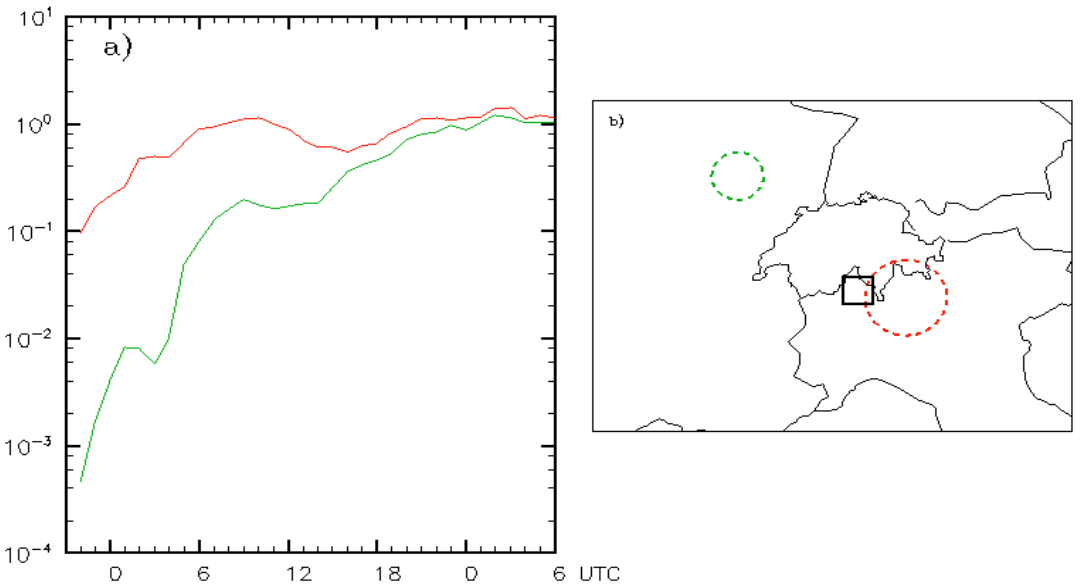

Figure 3. Vertical maximum absolute temperature difference between perturbed and control simulations averaged over the Simplon region for IOP2a. The location of the Simplon region and of the two initial Gaussian disturbances is shown on Fig. 3b.

The green curve on Fig. 3a is characterized by three growth phases, which can be related to different wave activities (see Hohenegger and Schär 2005a). The first exponential growth is triggered by the arrival of a sound wave, which was itself excited by the imposed initial temperature difference. Due to the small energy fraction carried by the sound wave and to the stability properties prevailing over the Simplon region, the first growth phase only lasts until 1 UTC. The second and third exponential increases visible on Fig. 3a are linked to the presence of gravity waves. Those were originally triggered by the sound wave over highly unstable regions and over the topography. Owing to their larger amplitude, they can cause error growth over less unstable regions, what further contributes to reduce the impact of the chosen sampling strategy.

Even if the presence of instabilities (respectively convection in the control simulation as in IOP2a) appears as a necessary factor for promoting error growth, this latter one often needs to be triggered by the presence of gravity waves (as over the Simplon region). In particular, only atmospheric flows sustaining the propagation of waves with relatively large group velocity (i.e. larger than the mean wind velocity), seem to be suited for such exponential growths and thus may disrupt the predictability level (see Hohenegger and Schär 2005b).

The combination of sound waves (to compensate for time lags) and of gravity waves (to compensate for amplitude differences) seems very effective in reducing the impact of different sampling strategies. It is clear, that the use of ad hoc perturbations (which might not project on the most unstable phase space)

and of perfect lateral boundary conditions combined with a relatively small integration domain, probably enhance the similarity between the different simulations. In particular, none of our simulations was able to develop its full own solution, as generally observed with larger-scale EPS. Since the synoptic situation could not be in-depth perturbed, and since this latter one seems a key factor in localizing error growth, similarity is ensured.

3. CONCLUSION

The sensitivity of artificially triggered perturbations has been studied by means of real-case simulations performed with the limited-area model LM. The comparison of the different simulations reveals a poor sensitivity of the locations of growing disturbances for larger discrepancies in their magnitude with regard to the chosen perturbation methodology. The presence of sound and gravity waves, the use of perfect lateral boundary conditions and the observed initial non-linearity of the system seem to favor the analogy between the different sampling techniques. From an operational point of view, the deduced non-linearity would prevent the use of singular vectors to construct an EPS on such scales, while the derived insensitivity would speak for the design of an EPS made of few members.

Acknowledgment: *The simulations were performed on the NEC SX-5 at the Swiss National Supercomputing Centre (CSCS) in Manno. The authors wish to acknowledge D. Lüthi for technical support and O. Fuhrer for discussions.*

REFERENCES

Ehrendorfer, M., 1997: Predicting the uncertainty of numerical weather forecasts: a review. *Meteor. Z.*, **6**, 147-183.

Hohenegger, C. , and C. Schär, 2005a: Sampling strategies in high-resolution short-range EPS and their impacts on the predictability level. *In preparation.*

Hohenegger, C., and C. Schär, 2005b: Dynamics of error growth in convection-resolving models. *In preparation.*

Steppeler, J., G. Doms, U. Schättler, H. Bitzer, A. Gassmann, U. Damrath, and G. Gregoric, 2003: Meso-gamma scale forecasts using the nonhydrostatic model lm. *Meteorol. Atmos. Phys.,* **82**, 75-96.

Walser, A., D. Lüthi and C. Schär, 2004: Predictability of precipitation in a cloud-resolving model. *Mon. Wea. Rev.*, **132**, 560-577.